Published in final edited form as:
Stem Cells. 2015 February ; 33(2): 601–614. doi:10.1002/stem.1867.

Human mesenchymal stromal cells attenuate graft-*versus*-host disease and maintain graft-*versus*-leukemia activity following experimental allogeneic bone marrow transplantation[1]

Jeffery J. Auletta, M.D.[1,2], **Saada K. Eid, B.S.**[3], **Patiwet Wuttisarnwattana, M.S.**[4], **Ines Silva, Ph.D.**[5], **Leland Metheny, M.D.**[6], **Matthew D. Keller, B.A.**[3], **Rocio Guardia-Wolff, B.S.**[3], **Chen Liu, M.D., Ph.D.**[7], **Fangjing Wang, Ph.D.**[6], **Theodore Bowen, B.A.**[3], **Zhenghong Lee, Ph.D.**[4], **Luis A. Solchaga, Ph.D.**[8], **Sudipto Ganguly, Ph.D.**[5], **Megan Tyler, B.A.**[5], **David L. Wilson, Ph.D.**[4], and **Kenneth R. Cooke, M.D.**[5]

[1]Host Defense Program, Hematology/Oncology/BMT and Infectious Diseases, Nationwide Children's Hospital, Columbus, OH 43205

[2]Department of Pediatrics, The Ohio State University, Columbus, OH 43205

[3]Department of Pediatrics, Case Western Reserve University, Cleveland, OH 44106

[4]Department of Biomedical Engineering Case Western Reserve University, Cleveland, OH 44106

[5]Department of Oncology, Sidney Kimmel Cancer Center, Baltimore, MD 21287

[6]Department of Medicine, Case Western Reserve University, Cleveland, OH 44106

[7]Department of Pathology, University of Florida School of Medicine, Gainesville, FL 32608

[8]Research & Development, Biomimetic Therapeutics, Franklin, TN 37067

Abstract

We sought to define the effects and underlying mechanisms of human, marrow-derived mesenchymal stromal cells (hMSCs) on graft-*versus*-host disease (GvHD) and graft-*versus*-leukemia (GvL) activity. Irradiated B6D2F1 mice given C57BL/6 BM and splenic T-cells and treated with hMSCs had reduced systemic GvHD, donor T-cell expansion, and serum TNFα and IFNγ levels. Bioluminescence imaging demonstrated that hMSCs redistributed from lungs to abdominal organs within 72h; and target tissues harvested from hMSC-treated alloBMT mice had less GvHD than untreated controls. Cryo-imaging more precisely revealed that hMSCs preferentially distributed to splenic marginal zones and regulated T-cell expansion in the white pulp. Importantly, hMSCs had no effect on *in vitro* cytotoxic T-cell activity and preserved potent

[1]Research was supported in part by funding from NIH grant AI 57801 (J.J.A.), the Center for Stem Cell and Regenerative Medicine at Case Western Reserve University (J.J.A. and K.R.C.), the Ohio Board of Regents (K.R.C.), and the Meredith Cowden Foundation (K.R.C.). Auletta and Eid co-first authors.

Corresponding author: Jeffery J. Auletta, M.D., 700 Children's Drive, Columbus, OH 43205; Phone: 614-722-3582; Fax: 614-722-3369; jeffery.auletta@nationwidechildrens.org.

Conflict-of-interest disclosure: The authors declare no competing financial interests.

Contributions: Conception and design (JJA, LAS, ZL, DLW, KRC), collection and/or assembly of data (SKE, LM, MDK, RGW, CL, FW, TB, PW, IS, SG, MT), data analysis and interpretation (JJA, KRC), manuscript writing (JJA, KRC), financial support (KRC), final approval of manuscript (all)

GvL effects *in vivo*. Mixed leukocyte cultures containing hMSCs exhibited decreased T-cell proliferation, reduced TNFα, IFNγ, and IL-10, but increased PGE_2 levels. Indomethacin and E-prostanoid 2 (EP2) receptor antagonisms both reversed while EP2 agonism restored hMSC-mediated *in vitro* T-cell suppression, confirming the role for PGE_2. Furthermore, cyclo-oxygenase inhibition following alloBMT abrogated the protective effects of hMSCs. Together, our data show that hMSCs preserve GvL activity and attenuate GvHD and reveal that hMSC biodistribute to secondary lymphoid organs wherein they attenuate alloreactive T-cell proliferation likely through PGE_2 induction.

Keywords

Mesenchymal stromal cells; graft-versus-host disease; graft-versus-leukemia

Introduction

Allogeneic bone marrow transplantation (alloBMT) is characterized by donor T-cell activation, which eradicates residual host malignant cells through immunologic mechanisms (graft-*versus*-leukemia, GvL activity) but often causes graft-*versus*-host disease (GvHD) [1]. GvHD and malignant disease relapse remain the primary causes of death following alloBMT [2]. Therefore, novel therapies that modulate alloreactivity without compromising GvL activity are critically needed to improve outcomes and to broaden therapeutic application of alloBMT [3].

Human multipotent mesenchymal stromal cells (hMSCs) are non-hematopoietic, adult progenitor cells that can be expanded from numerous tissue sources and have the ability to differentiate into bone marrow stroma as well as adipocytes, chondrocytes and osteocytes [4]. In addition to producing soluble proteins that critically support hematopoietic stem cell homeostasis and engraftment [5–7], hMSCs possess immunomodulatory properties [8]. Specifically, hMSCs have been shown to inhibit *in vitro* T-cell activation and function through soluble factors like IDO, IL-10, TGFβ, hepatocyte growth factor (HGF), and prostaglandin E2 (PGE_2) [9]. Given their immunosuppressive properties, ease in expansion, and safe infusion profile [10], MSCs have been used for steroid-refractory acute GvHD [11]. Yet the bio-distribution and mechanisms underlying *in vivo* MSC effects remain largely undefined [12, 13], contributing to mixed clinical results and tempered enthusiasm for the use of hMSCs after alloBMT [14].

We used an established alloBMT model to elucidate the *in vivo* immunomodulatory effects of hMSCs on donor T-cell responses. Murine BMT models have helped define mechanisms contributing to stem cell engraftment, immune reconstitution, GvHD, and GvL activity [15]. Likewise, murine xenogeneic transplant models should be useful in defining *in vivo* hMSC-mediated immunosuppression since hMSCs have low immunogenicity, lack MHC class II and co-stimulatory molecule expression, and fail to activate T-cells *in vitro* [16], all key features that allow their use in MHC-mismatched transplantation [17]. We specifically chose to study hMSCs given the multiple differences in immunomodulatory effects between human and murine MSCs [18]. For example, murine MSCs require cell-to-cell contact,

whereas hMSCs can mediate immunosuppression through soluble factors [19, 20]. Secondly, murine MSCs induce *in vitro* T-cell anergy [21], whereas hMSCs do not induce T-cell anergy or apoptosis [22]. Finally, murine MSCs inhibit *in vitro* T-cell alloreactivity through inducible nitric oxide synthase (iNOS) [23], whereas hMSCs utilize IDO [24]. We tested the hypothesis that hMSCs would attenuate GvHD and preserve GvL activity in mice after alloBMT. In addition to using *in vitro* immune assays and *in vivo* models of GvHD and GvL, we used novel *in vivo* imaging to interrogate hMSC biodistribution. Novel microscopic cryo-imaging (CryoViz™, BioInVision, Inc.) with single cell sensitivity was used to quantify hMSC homing to the spleen and hMSC effect on T-cell proliferation and expansion.

Materials and Methods

Mice and bone marrow transplantation

All animal studies were approved by the Institutional Animal Care and Use Committee (IACUC) at Case Western Reserve University (IACUC protocol 2010-0076). Female C57BL/6J (B6; H-2^b) and B6D2F1 (F1; H-2^{bxd}) mice aged 8 to 12 weeks were purchased from Jackson Laboratory (Bar Harbor, ME). B6D2F1 (H-2^{bxd}) mice received 14 Gy (split dose) total body irradiation (TBI) prior to receiving BM and splenic T-cells from either naïve allogeneic B6 or syngeneic B6D2F1 donors. Bone marrow (5 million, 5M) and T-cells (2M) were suspended in 200 μl Leibovitz L-15 media and injected intravenously into recipient mice on day 0 (D0) [25]. T-cell purification was performed by magnetic-bead separation using MicroBeads and the autoMACS system (Miltenyi Biotec, Auburn, CA) with more than 85% of cells obtained being positive for CD4 or CD8 surface antigens. On 1 (D1) and 4 (D4) days post-BMT, 1M culture-expanded, BM-derived human MSCs were administered by tail-vein injection. In indicated experiments, indomethacin (20 μg ≈ 1 mg/kg, Sigma-Aldrich, St. Louis, MO) was administered as a daily intraperitoneal injection (100 μg/ml) for 7 days starting on D1. Pilot experiments (conducted without MSC infusions) using this dose and schedule demonstrated that indomethacin had no significant effects on survival when administered to allogeneic and syngeneic BMT mice compared to controls in each group (data not shown).

Culture and expansion of human bone marrow-derived mesenchymal stem cells, MSCs

Human MSCs were derived from BM aspirates from healthy donors [26]. Patients were consented for the procedure in accordance with the Institutional Review Board of University Hospitals Case Medical Center (UHCMC IRB protocol 09-90-195). Specimens were collected and processed by the Hematopoietic Stem Cell Facility of the Case Comprehensive Cancer Center. Adult volunteer donors underwent BM aspiration (10–30 ml) under local anesthesia. Mononuclear cells were isolated by Percoll gradient centrifugation (1.073 gm/ml) and plated at a density of 1.7×10^5 cells/cm^2 in 175 cm^2 tissue culture flasks in complete MSC medium [DMEM low glucose, supplemented with 1% antibiotic/antimycotic, and 10% fetal bovine serum from selected lots; all reagents from Gibco-Invitrogen, Carlsbad, CA]. Cells were allowed to adhere for 72 h followed by removal of non-adherent cells and media changes every 3 to 4 days. When cultures reached 80–90% confluency, adherent cells were subcultured by trypsinization, counted and re-plated at a density of $2–6 \times 10^3$ cells/cm^2 per 175 cm^2 (“passage”). Third- to fifth-passage hMSCs were

used in the functional assays below, and hMSC phenotype was confirmed by morphology, flow cytometry ($CD45^{-}CD105^{+}CD90^{+}CD80^{-}CD73^{+}HLA\text{-}I^{+}$), and *in vitro* differentiation into osteoblasts, chondroblasts and adipocytes [4].

Assessment of acute GvHD

Prior to transplant, recipient transplant mice were ear punched and weights were obtained and recorded on D0 and weekly thereafter. Survival was monitored daily, and the severity of systemic GvHD was assessed weekly using a semi-quantitative scoring system that incorporated five clinical parameters (two points each, maximum score = 10): weight loss, posture (hunching), activity, fur texture, and skin integrity [25]. Acute GvHD was also assessed by histopathology of the liver, ileum, and ascending colon in blinded fashion by a single pathologist [27] as previously described [25].

Bioluminescence imaging

hMSCs were transduced using a lentiviral vector with a reporter system that allows both qualitative and quantitative longitudinal imaging of cell transplants in small animal models as described [28]. The triple-fusion reporter *fluc-mrfp-ttk* (LRT; a gift from Sam S. Gambhir, Stanford University) encodes a fusion protein containing functional components from firefly luciferase (*fluc*), whose reporter gene product can be visualized using bioluminescence imaging (BLI). Viral transduction of hMSCs with the triple reporter gene has no effect on multipotent characteristics of MSCs [28]. After receiving transduced MSCs via tail-vein injection, mice were imaged by BLI. Each mouse was anesthetized with isoflurane administrated by using an EZ-Anesthesia system (Euthanex, Allentown, PA) and restrained in a horizontal position after induction. Five minutes before the scan, animals were given intraperitoneal injection of 0.2 mg of D-luciferin in 0.2 mL of sterile PBS. Imaging was subsequently performed using a Xenogen IVIS 200 System (Caliper/Xenogen, Hopkinton, MA) equipped with a cooled CCD camera and with a 3-min exposure time 6 minutes after D-luciferin injection. In some experiments, BLI images were acquired on the IVIS Spectrum Pre-clinical In Vivo Imaging System (Perkin Elmer, Alameda, CA), and at designated time-points, organs (spleen and liver) were harvested from luciferin-injected mice and imaged *ex vivo*. Images were analyzed with Living Image Software 4.4 (Perkin Elmer) and data quantified as photons/second [29].

Cryo-imaging

All animals used in cryo-imaging experiments received alfalfa-free chow for two weeks prior to BMT to reduce background fluorescence in the gastrointestinal tract. hMSCs were fluorescently-labeled with red quantum dots (70% efficiency verified by flow cytometry), and 1M cells were infused on D1 following allogeneic and syngeneic BMT as described above. In some experiments, splenic T-cells from donor C57BL/6 mice were fluorescently labeled with CFSE dyes [30] (100% efficiency verified by flow cytometry) and infused into syngeneic and allogeneic transplant mice on D0 followed by infusion of labeled hMSCs on D1. Ultimately, four experimental groups were defined: (1) syngeneic mice given no hMSCs (“syn”); (2) syngeneic mice given hMSCs (“syn + MSC”); [31] allogeneic mice given no hMSCs (“allo”); and (4) allogeneic mice given hMSCs (“allo + MSC”). Mice were

sacrificed at 24, 48, 72, 96 and 120 h after BMT, embedded en bloc in optimal cutting temperature (OCT) compound, snap frozen in liquid nitrogen, and ultimately imaged. In some experiments individual organs were collected at the specified time points and cryopreserved separately before imaging.

The cryo-imaging device (CryoViz™, BioInVision, Inc.) is a fully-automated, whole mouse section-and-image system which provides 3-dimensional, tiled, microscopic anatomical bright field and molecular fluorescence image over vast volumes [32]. Mice were sectioned at 40 μm and imaged at 10.5 × 10.5 μm in plane resolution. With sufficient sensitivity for detection of single cells, cryo-imaging permits unique quantitative analyses of fluorescently-labeled cells using specialized image analysis and visualization software [33]. We used specialized algorithms to allow detection of both fluorescent green T-cells and red hMSCs were developed. Briefly, fluorescent images were pre-processed to remove highly autofluorescent structures like food remnants in the gastrointestinal tract and skin. Filters were used to extract features, and a machine-learning, "bagged decision tree" classifier was used to detect cells. Connected components were used to extract intensity profiles for each individual cell. Interactive image segmentations were used to segment organs and tissues of interest such as the spleen and white pulp. Since CFSE dye intensity per cell decreases with T-cell clonal expansion, intensity histogram analysis of T-cells was used to provide an assay for *in vivo* T-cell proliferation assay [34]. In experiments, the percentage of T-cells retaining high CFSE signal was measured from the histogram.

Mixed leukocyte culture (MLC)

Spleens harvested from individual mice were enzymatically digested into single cell suspensions. Purified splenic T-cells (B6 mice) or dendritic cells (B6D2F1 mice) were suspended in supplemented 10% FCS/RPMI. B6 T-cells (2×10^5) were cultured in 96-well plates in the presence of B6 or B6D2F1 splenic $CD11c^+$ dendritic cells (2×10^4 DCs) at 37°C in a humidified incubator supplemented with 7% CO_2. After 72 or 96 h, supernatants were obtained from individual wells and subsequently analyzed for cytokines by ELISA. Proliferation was measured by incorporation of tritiated thymidine [^{3}H] (3.7037×10^4 Bq) during the last 24 h of incubation using a 1205 Betaplate reader (Wallac, Turku, Finland). In indicated experiments, hMSCs were added to MLC wells at MSC-to-T-cell ratios ranging from 1:1 through 1:32 with and without indomethacin (1 μg/ml, Sigma), the EP2 agonist, butaprost (BT, 2 μg/ml, Cayman Chemicals), and the EP2 antagonist, PF-04418948 (PF, 2 μg/ml, obtained from Pfizer with permission). Specifically, PF and BT were used in MLCs at lower hMSC-to-alloreactive T-cell ratios to approach the limit of measurable hMSC-mediated immune suppression via PGE_2 induction.

CTL activity

CTLs were generated following stimulation of B6 T-cells (2×10^6) with F1 splenic DCs (2×10^5) in primary bulk MLCs (24-well plates, BD Biosciences, San Diego, CA) for 4 days. T cells were isolated by Ficoll gradient, and subsequently added to 96-well plates (starting with 4×10^4 T-cells/well and then serial two-fold dilutions) with ^{3}H-labeled P815 ($H\text{-}2K^d$) or EL4 ($H\text{-}2K^b$) target cells (1×10^3 cells with starting 40:1 CTL-to-target ratio). Wells containing target cells only (total count well, T) were used to determine spontaneous ^{3}H

release (S); S = [(T-S)/T] × 100. After 4 h, cells were harvested from experimental (E) wells containing target cells and serially-diluted T-cells and assayed for ^{3}H release. Percent cytotoxicity was calculated as [(S-E)/S] × 100.

In vivo leukemia challenge

P815 (H-2K^{d}, CD45.2) is a mastocytoma cell line derived from DBA/2 mice. Injection of P815 cells into syngeneic mice (H-2K^{d}) is uniformly lethal and results in massive tumor infiltration and enlargement of the liver and spleen with characteristic nodule formation [35]. In GvL experiments, B6Ly5.2 (CD45.1) mice were used as alloBMT donors and 500 P815 tumor cells were added to the BM inoculum on D0, a time that ensures viable leukemia cells are not affected by the cytotoxic effects of TBI and immediately before the time hMSCs influence alloreactive T-cell proliferation and expansion. Survival was monitored daily, and post-mortem examination defined the cause of death after BMT as either GvHD or tumor [25]. Minimal residual disease (MRD) was determined by FACS analysis of spleen cells collected on D13 and also following necropsy of animals without gross evidence of organ tumor infiltration. Flow cytometric evaluation at D42 and D70 provided a cost effective and rigorous assessment for the presence of MRD in late post-alloBMT surviving animals. This GvL mouse model has been instrumental in translational application of novel agents for the treatment or prevention of GvHD [36–39].

Flow cytometry

Splenocytes were analyzed pre-transplant or on D10 unless otherwise specified. Splenic cell suspensions were stained for surface T-cell (CD4, CD8) and activation markers (CD25, CD28, CD62L, CD69) along with T-cell intracellular TNFα and IFNγ, and then analyzed by flow cytometry using a 4-color C6 FlowCytometer (Accuri, Ann Arbor, MI) as previously described [25]. To analyze FoxP3 expression, splenocytes were stained with anti-CD4 and anti-CD25, fixed and permeabilized, and then stained with intracellular anti-FoxP3 (eBioscience, San Diego, CA). All mAbs were purchased from BD Biosciences Pharmingen (San Diego, CA) or eBioscience. Irrelevant fluorochrome rat isotype control immunoglobulins were used as negative controls. At least 1×10^{4} events were analyzed per conjugated mAb stain condition. Data was analyzed suing CFlow software (Accuri, Ann Arbor, MI).

ELISA

Peripheral blood was collected on D7 and D10 from BMT recipients in 1.1-mL Z-Gel serum separation microtube (Sarstedt, Newton, NC). Following serum separation, ELISA was performed. MLC supernatants were harvested at 48 or 72h as indicated and then assayed for mouse cytokines (IL-10, TGF-β1, IFNγ, PGE_2, TNFα) according to manufacturer instructions (R&D Systems, Inc. and eBioScience).

Immunohistochemistry (IHC)

Formalin-fixed, paraffin-embedded, and slide-mounted sections were boiled in citrate buffer (pH 6.0) for antigen retrieval. For β-2-microglobulin staining, sections were incubated one hour at room temperature with a 1:80 dilution of monoclonal, mouse, anti-human β-2-

microglobulin antibody (Novus Biologicals, Littleton, CO) and binding was detected by M.O.M. Immunodetection Peroxidase Kit (Vector Laboratories, Burlingame, CA) following manufacturer's instructions. Counterstaining was completed with hematoxylin.

Statistics

All values are expressed as the mean plus or minus standard error of the mean (± SEM). Statistical comparisons between groups were completed using the Mann-Whitney test (non-parametric data) and unpaired *t*-test (parametric data). For survival curves, the Mantel-Cox log-rank test was used. Statistical significance was defined as a *p*-value less than 0.05 using relevant statistical analyses in GraphPad Prism Software (La Jolla, CA).

Results

Human bone marrow-derived MSCs infusions attenuate T-cell expansion and pro-inflammatory cytokine induction and improve survival after experimental alloBMT

To interrogate the *in vivo* effects of hMSCs during GvHD, we used an established alloBMT model (B6→B6D2F1). Recipients of syngeneic BMT (F1→F1) served as controls. One million hMSCs were administered via tail-vein on D1 and D4 after BMT on D0. Human MSCs had a significant effect on the severity of systemic GvHD as measured by D42 survival (Figure 1A) and weekly clinical scores. For example, D28 mean clinical scores for hMSC-treated transplant mice were less than measured for untreated transplant recipients (3.4 ± 0.4 *vs.* 2.2 ± 0.3, respectively, $p < 0.01$) and these differences persisted through D42 (Figure 1B). In this alloBMT model, maximal donor T-cell expansion is observed between D7 and D14 [25, 37–40] after BMT. Therefore, we analyzed mouse splenocyte T-cell populations at D10 to determine if hMSC infusions reduced the number of donor T-cells present in the spleen early after BMT. AlloBMT recipients showed significant increases in donor $CD4^+$ and $CD8^+$ T-cells in the spleen compared to syngeneic controls (Figure 1C). Injection of hMSCs after alloBMT significantly reduced splenic T-cell numbers. Next, we compared serum levels of proinflammatory cytokines. AlloBMT mice had significantly higher levels of circulating IFNγ and TNFα than syngeneic controls. However, alloBMT mice receiving hMSCs had nearly 50% reduction in circulating IFNγ (Figure 1D) and TNFα (Figure 1E) levels compared to untreated alloBMT controls. Reductions in circulating levels of IFNγ and TNFα correlated with decreased cytokine-producing $CD4^+$ and $CD8^+$ splenic T-cells in MSC-treated alloBMT mice (data not shown).

Human MSCs redistribute to abdominal organs and reduce tissue inflammation

We next determined whether target organ integrity was preserved in MSC-treated alloBMT mice. First, we used bioluminescence imaging (BLI) to define if hMSCs, lentiviral-transduced with a triple-fusion, firefly luciferase reporter gene, could be detected in GvHD target organs [28]. Transduced hMSCs (t-hMSCs) initially tracked to the pulmonary circulation and then redistributed to intra-abdominal organs of alloBMT recipient mice within 72 h of infusion (Figure 2A). In contrast, t-hMSCs injected into syngeneic mice tracked to the pulmonary circuit only. By Day 10, evidence for hMSCs in the intestinal track was confirmed by evaluation of organs post-necropsy by *ex vivo* BLI (Figure 2B) and microscopically using immunohistochemistry (IHC) for reporter expressing cells (data not

shown). Target organs (liver, small and large bowel) from BMT mice at D10 demonstrated appreciable differences in histopathology (Figure 2C). Specifically, hMSC-treated alloBMT mice exhibited significantly lower histology scores than untreated alloBMT mice (Figure 2D).

Human MSCs home to the spleen and attenuate in vivo T-cell proliferation

Secondary lymphoid organs (SLO) like the spleen are important sites of donor T cell activation and expansion during alloBMT [41, 42]. As hMSCs significantly attenuated splenic T-cell proliferation and BLI showed evidence for redistribution of cells into abdominal organs, we next used cryo-imaging technology to determine if hMSCs might co-localize with alloreactive T-cells in spleen during GvHD induction [32]. BMT recipients were first tail-vein injected with 1M fluorescently-labeled (Qtracker 625 red quantum dots) hMSCs on D1. Mice were sacrificed and snap frozen for cryo-imaging at several time points. Six hours after infusion, fluorescent cryo-imaging with single-cell resolution demonstrated that the majority of Qdot-labeled hMSCs were found in the lung (83%) and liver (17%) (Figure 3A). Single-cell tracking showed that hMSCs re-distributed from the lung to the liver and spleen by 24 h post-injection (D2 after BMT) (Figures 3B and 3C). Upon closer examination, hMSCs migrated specifically to splenic marginal zones (Figures 3D and 3E), and greater numbers of hMSCs were found in the spleens of allogeneic as compared to syngeneic controls at all-time points including 96 h (D4 after BMT) (Figure 3E through 3J). The presence of hMSCs in the spleens of allo-BMT recipients was confirmed using two additional methods: IHC using human β-2- microglobulin and BLI since only intact cells should be bioluminescent in response to luciferin. As shown in figure 3, panels K and L, the presence of hMSCs was detected by each method 4 to 5 days after injection.

To study the biologic significance of these findings, CFSE-labeled donor lymphocytes were infused on D0 followed by infusion of Qdot-labeled hMSCs on D1. Cryo-imaging analysis at 48, 72, and 96 h after BMT revealed that T cells in alloBMT mice given hMSCs retained their CFSE fluorescence intensity to a degree greater than allogeneic mice not given hMSCs, but less than minimally proliferating syngeneic T cells (Figure 4A and 4B). Correspondingly, whole spleen and white pulp volumes were also reduced in alloBMT mice receiving hMSCs (Figure 4C). Taken together with data in figure 1C, these findings show that early after infusion, hMSCs track to the splenic marginal zone in alloBMT recipients and regulate alloreactive T-cell proliferation and resultant expansion in white pulp.

Human MSCs modulate in vitro murine T-cell activation and cytokine secretion

To define the capacity and mechanism by which hMSCs exert their immunosuppressive effects, we next tested their ability to suppress T-cell proliferation in MLCs. Human MSCs were co-cultured with B6 T-cells and either B6 or B6D2F1 dendritic cells (DCs). Human MSCs (Figure 5A), but not human fibroblasts (Figure 5B), significantly inhibited murine T-cell proliferation in a concentration-dependent manner, confirming that immunomodulation is unique to hMSCs. Consistent with previous work [43], supernatants collected from hMSCs first stimulated with either IL-1β or human peripheral blood mononuclear cells (PBMNC) also showed concentration-dependent suppression of T-cell alloreactivity (Figure 5C). These

data suggest that hMSCs activated by pro-inflammatory cytokines and other immune effector cells produce immunomodulatory soluble factors that suppress T-cell proliferation.

We next examined the effects of hMSCs on cytokine secretion. The addition of hMSCs significantly decreased levels of inducible TNFα, IFNγ and IL-10 in MLC supernatants (Figure 5D). Subsequent evaluation of immunomodulatory cytokines (PGE_2 and TGFβ1) known to mediate hMSC T-cell suppression [9, 43] revealed that levels of PGE_2 and TGFβ1 were significantly elevated by nearly 4- and 7-fold, respectively, in supernatants from MLC cultures containing hMSCs (Figure 5D). Lastly, we found that the $CD4^+CD25^+FoxP3^+$ T-regulatory content was also elevated compared to MLCs without hMSCs, but not to the point of statistical significance (33.4 ± 9.8 *vs.* 13.8 ± 1.9%, respectively, $p = 0.066$, n = 3 separate experiments).

The role of PGE_2 in hMSC-mediated suppression of mouse T-cell alloreactivity and survival advantage following alloBMT

We next examined the role that PGE_2 played in hMSC-mediated immunosuppression observed in our experimental systems. In MLCs containing MSCs, addition of indomethacin (IM), a cyclooxygenase (COX) inhibitor known to inhibit PGE_2 production, significantly reversed both inhibition in T-cell proliferation (Figure 6A), attenuation in surface $CD28^+$ and $CD69^+$ expression (Figure 6B) and increases of CD62L expression (data not shown) in both $CD4^+$ and $CD8^+$ T-cells. PGE_2 signals through four different receptors (EP1, EP2, EP3 and EP4), which have variable affinity for PGE_2. Specifically, low-affinity EP1 and EP2 require higher concentrations of PGE_2 than higher-affinity EP3 and EP4 for effective signaling [44]. In this regard, the EP2 antagonist, PF-04418948 (PF), and agonist, Butaprost (BT), were used to refine further the effects of PGE_2 in modulating T-cell proliferation. At lower levels of PGE_2 induction, addition of IM again restored T-cell proliferation in the presence of hMSCs (Figure 6C). PF-induced EP2 blockade also significantly reversed inhibition in T-cell proliferation by hMSCs, albeit not to the same degree as direct COX inhibition (Figure 6C). Next, we found that addition of BT to MLCs fully reversed the effects of IM on hMSC immunomodulation, suggesting that despite absent induction of a COX-dependent factor, direct ligation of the EP2 receptor was sufficient to mediate MSC effects on T-cell proliferation (Figure 6C). Given these *in vitro* effects of IM, we treated hMSC-treated alloBMT mice with daily IM for seven consecutive days (D1–D7) and observed reversal in survival advantage conferred by hMSCs (Figure 6D). Together, these results suggest that the measured effects of hMSCs on alloreactive T-cell proliferation are mediated in large part through PGE_2.

In vitro tumor cell lysis and graft-versus-leukemia activity in alloBMT mice are maintained in the presence of human MSCs

Our data demonstrate that hMSCs exert potent regulatory effects on *in vivo* T-cell alloreactivity. Therefore, we were interested in determining whether hMSC infusions would negatively impact GvL activity after alloBMT. We first assessed effects of hMSCs on cytolytic activity of murine cytotoxic lymphocytes (CTLs) generated *in vitro* and found that the presence of hMSCs during CTL generation had no effect on the ability of B6 CTLs to lyse P815 tumor targets on a per cell basis (Figure 7A). Likewise, alloBMT mice receiving

hMSC infusions maintained a survival advantage over untreated alloBMT mice even after *in vivo* challenge with P815 (Figure 7B). As expected, syngeneic control mice receiving P815 experienced rapid demise from fulminant tumor progression by D21. By contrast, rejection of tumor occurred in alloBMT mice, but they ultimately died from GvHD sooner than hMSC-treated alloBMT. Importantly, levels of minimal residual disease (MRD) in the spleen at D14 (Figure 7C) and at days D42 and D70 (Figure 7D) were similar between MSC-treated and untreated alloBMT mice, suggesting that hMSCs did not abrogate *in vivo* GvL activity. Similar findings were observed even when donor T-cell doses were reduced by 50% in alloBMT mice co-infused with BM and P815 tumor cells (Figure 7D).

Discussion

Success in using hMSCs to prevent or to treat GvHD and other inflammatory disorders has been limited by an incomplete understanding of the bio-distribution and mechanism of action of these cells [12, 13, 45]. To begin to address these limitations, we used an established, clinically relevant murine alloBMT model to measure the *in vivo* effects of hMSCs on T-cell alloreactivity. We specifically chose to study hMSCs given the inherent differences in expansion, proliferation and immunosuppression between human and murine MSCs [46, 47] as well as the differences in immunologic function across species [18, 48]. Potent immune-regulatory activity was observed in association with the co-localization of hMSCs with alloreactive T-cells within the spleen. These effects correlated with decreased levels of circulating TNFα and IFNγ and resulted in reduced systemic and target organ GvHD following alloBMT. Correlative *in vitro* studies revealed that PGE_2 plays a critical role in hMSC-mediated attenuation in alloreactive T-cell activation and proliferation and administration of indomethacin during alloBMT reverses the protective *in vivo* effects of hMSCs. Finally, hMSC infusions did not negatively impact GvL activity; as hMSC-treated, P815-challenged alloBMT mice maintained survival advantage compared to untreated alloBMT mice and had no differences in detectable MRD even in the context of reduced donor T-cell content.

Xenogeneic mouse models have been used to define a variety of human immune responses [49]. With respect to hMSC immunomodulation, xenogeneic models have shown that adipose tissue- [50], umbilical cord blood- [51], and BM-derived [52] hMSCs can successfully prevent or treat GvHD. One unifying theme among xenogeneic models is that hMSC therapy is most effective when administered in the early post-transplant period, suggesting that an inflammatory milieu is needed to activate MSC function. Inflammatory-mediated activation of MSC function was first suggested by *in vitro* studies incorporating IL-1β [43] and IFNγ [53] and later further defined using murine models of GvHD induction. Specifically, IFNγ was found to be necessary in activating MSC-mediated immunosuppression and that MSCs pre-treated with increasing concentrations of IFNγ prevented GvHD in a dose-dependent manner [54]. Similarly, IFNγ in combination with IL-1α, IL-6, and TNFα within the microenvironment induced MSCs to produce T-cell chemotactic chemokines (CXCL-9 and 10) in order for nitric oxide (NO) produced by activated MSCs to then inhibit T-cell alloreactivity [23]. Finally, delay in hMSC administration post-PBMNC infusion conferred protection against development of xenogeneic GvHD, suggesting that timing of hMSC infusion was critical to allow *in vivo* activation of MSC-mediated immunosuppression [52]. In

our current studies, hMSCs were injected into recipient mice at days 1 and 4 following alloBMT, an established time for T-cell expansion and pro-inflammatory cytokine induction [25]. IFNγ does not show cross-species reactivity, so mouse and human cells do not bind nor are sensitive to IFNγ of the other species [55]. Therefore, other pro-inflammatory factors are likely responsible for the activation of MSC function in our studies. *In vitro* experiments showed that soluble factors produced by hMSCs pre-stimulated with either IL-1β or PBMNC potently suppress T-cell proliferation, further corroborating that hMSCs can be activated [13] or licensed [56] by their microenvironment.

It is important to note that GvHD can rarely occur after solid organ transplantation (SOT) and is driven primarily by alloreactive donor memory T cells [57–59]. Furthermore, recent literature suggests that HCT using stem cells from the solid organ donor prior to SOT may alleviate the risk for acute organ rejection as well as the need for long-term immunosuppression [60, 61]. Similarly, hMSCs have been utilized in animal models [62] as well as early phase clinical trials to induce tolerance on both local (solid organ) and systemic levels [63, 64]. Our experiments show that hMSCs attenuate GvHD induction by suppressing in vitro and in vivo donor T-cell alloreactivity and proliferation without compromising GvL. It remains to be determined if MSCs may function in a similar manner to mitigate GvHD occurring in the context of SOT.

Our data support a pivotal role for PGE_2 in the regulation of *in vitro* and *in vivo* T-cell alloreactivity consistent with many [65–67], but not all [68] reports studying hMSC effects on human T-cell alloreactivity. PGE_2 likely mediates hMSC immunosuppression [9, 69] through its heterogeneous effects on T-cell proliferation [68], Treg induction [70], and DC differentiation and maturation [71]. Furthermore, TGFβ1 and PGE_2 have established roles in both Treg- and MSC-mediated immunomodulation. For example, TGFβ1 [72] and PGE_2 [70] expand Treg cells via induction of FoxP3 within $CD4^+CD25^-$ precursors. Human MSCs can also induce *in vitro* $CD4^+CD25^+FOXP3^+$ Treg cells [9] via non-redundant roles of MSC-derived TGFβ1 and PGE_2 [73]. However, Treg induction does not seem to mediate the *in vivo* effects of hMSCs in protecting against xenogeneic GvHD, wherein direct inhibition of donor $CD4^+$ T-cell proliferation and subsequent reduction in circulating TNFα are present without significant Treg induction [52]. Our results support this literature, as TGFβ1, PGE_2 and Treg induction were measured in MLCs containing hMSCs, although Treg induction was not consistently measured in splenocytes from hMSC-treated alloBMT mice (data not shown). Furthermore, IM significantly reversed *in vitro* MSC-mediated suppression of T-cell proliferation and activation as well as the survival advantage noted in hMSC-treated alloBMT mice.

Xenogeneic studies have also shown that MSCs migrate to classic GvHD target organs, which demonstrate reduced tissue cytotoxicity upon histologic evaluation [50, 74]. Most imaging studies demonstrate that MSCs initially and transiently accumulate in the lungs. Subsequent organ-specific homing has been demonstrated in response to chemokine gradients [75] and tissue injury [76], and MSCs can attach to damaged endothelial cells via selectin and integrin binding [77]. Whether the reduced gastrointestinal GvHD found in our experiments is a reflection of local microenvironment changes induced by hMSCs themselves, hMSC regulation of effector T-cell expansion and cytotoxic cytokine production in secondary lymphoid organs, or a combination of both processes is currently under

investigation. Our findings favor a more primary role for MSCs on donor T cell activation, consistent with a recent study demonstrating the importance of CCR7 in guiding the migration of MSCs into secondary lymphoid tissues after alloBMT [78]. Moreover, once localized to the GvHD target tissue microenvironment, MSC-associated protective effects are likely to be more immunomodulatory rather than regenerative in nature [79], as evidence for direct tissue repair by hMSCs following clinical alloBMT is lacking [80, 81].

BLI from our experiments shows redistribution of hMSCs into abdominal organs within days following injection. Furthermore, whole-mouse cryo-imaging clearly demonstrates that hMSCs migrate to the liver and the spleen within 24 h after administration, Subsequently, human MSCs accumulate in the marginal zone of the spleen, co-localize with alloreactive T-cells in the splenic white pulp, and attenuate alloreactive T-cell proliferation and expansion. These results provide crucial insight connecting bio-distribution with local regulatory effects of hMSCs, which may ultimately reduce systemic cellular and soluble inflammatory mediators within the transplant recipient.

MSC-mediated immunosuppression or induced tolerance could favor tumor growth as suggested in experimental [82, 83] and clinical [84] reports and reviewed in [31]. Given these observations, we studied whether hMSCs would adversely affect GvL activity. We found that this critical protective effect was preserved both *in vitro* and *in vivo*. Furthermore, GvL activity was maintained despite reduced donor graft T-cell doses and continued to associate with amelioration in systemic GvHD in contrast to recent experience using adipose-derived murine MSCs [85]. These results extend the observation that host tolerance seems to be specific to donor MSCs themselves and not generalized to donor HLA immunogenicity [86] and further support recent clinical experience using MSCs in haploidentical [87] and nonmyeloablative [88] transplant settings in which GvL potency was maintained.

Summary

The current studies confirm and significantly extend previous findings regarding the immunomodulatory capacity of hMSCs. Our data show that hMSCs administered early after alloBMT attenuate systemic and target-organ GvHD in a haplo-identical mouse model. To our knowledge, our observations are the first to show that hMSCs home to the marginal zone of the spleen and regulate donor T-cell expansion in a manner that preserves allo-specific GvL response. These key findings create a platform from which future lines of investigation can be launched. For example, it remains to be determined whether hMSCs exert their effects on *in vivo* T-cell expansion directly via PGE_2 as suggested by our *in vitro* results and those reported in other human studies or indirectly via polarization to “MSC2” cells [89] and subsequent activation of resident splenic macrophages/monocytes to secrete IL-10 [90]. We were not able to observe a significant contribution for indoleamine 2, 3-dioxygenase (IDO) in MSC-mediated suppression of alloreactive T cell proliferation *in vitro* (data not shown), consistent with recent work demonstrating that modulation of T cell effector activity by IFNγ-licensed hMSCs is independent of IDO activity [91]. However, IDO has been shown to suppress T cell responses and promote tolerance in other settings, so studies to further evaluate the role of this molecule and other immunomodulatory soluble factors *in vivo* may have merit [92]. Similarly, whether strategies to expedite MSC homing to

secondary lymphoid tissue [9378] or to protect MSCs from various cytolytic mechanisms [94] will enhance efficacy MSC therapy also remain unstudied areas for investigation. Collectively, these inquiries will begin to address critical needs for investigation into the *in vivo* mechanisms of hMSC immunomodulation and for potential biomarkers of hMSC effects, both of which likely will impact the clinical efficacy of these cells in the clinical setting.

Acknowledgments

The authors wish to acknowledge the Hematopoietic Stem Cell Core Facility of the Case Comprehensive Cancer Center for its collection and processing of patient samples (P30 CA 43703), the National Center for Stem Cell and Regenerative Medicine at Case Western Reserve University for its continued research support, and Debashish Roy and Madhusudhana Gargesha at BioInVision, Inc. Mayfield Village, OH for their assistance in cryoimaging. The EP2 antagonist, PF-04418948, was kindly supplied by Pfizer.

References

1. Barrett AJ. Understanding and harnessing the graft-versus-leukaemia effect. Br J Haematol. 2008; 142:877–888. [PubMed: 18564358]
2. Pasquini, MC.; Wang, Z. Current use and outcome of hematopoietic stem cell transplantation: CIBMTR Summary Slides, 2012. 2012. Available at: http://www.cibmtr.org
3. Auletta JJ, Cooke KR. Bone marrow transplantation: new approaches to immunosuppression and management of acute graft-versus-host disease. Curr Opin Pediatr. 2009; 21:30–38. [PubMed: 19242239]
4. Dominici M, Le Blanc K, Mueller I, et al. Minimal criteria for defining multipotent mesenchymal stromal cells. The International Society for Cellular Therapy position statement. Cytotherapy. 2006; 8:315–317. [PubMed: 16923606]
5. Caplan AI, Dennis JE. Mesenchymal stem cells as trophic mediators. J Cell Biochem. 2006; 98:1076–1084. [PubMed: 16619257]
6. Mendez-Ferrer S, Michurina TV, Ferraro F, et al. Mesenchymal and haematopoietic stem cells form a unique bone marrow niche. Nature. 2010; 466:829–834. [PubMed: 20703299]
7. Le Blanc K, Samuelsson H, Gustafsson B, et al. Transplantation of mesenchymal stem cells to enhance engraftment of hematopoietic stem cells. Leukemia. 2007; 21:1733–1738. [PubMed: 17541394]
8. English K. Mechanisms of mesenchymal stromal cell immunomodulation. Immunol Cell Biol. 2013; 91:19–26. [PubMed: 23090487]
9. Aggarwal S, Pittenger MF. Human mesenchymal stem cells modulate allogeneic immune cell responses. Blood. 2005; 105:1815–1822. [PubMed: 15494428]
10. Lalu MM, McIntyre L, Pugliese C, et al. Safety of cell therapy with mesenchymal stromal cells (SafeCell): a systematic review and meta-analysis of clinical trials. PLoS One. 2012; 7:e47559. [PubMed: 23133515]
11. Le Blanc K, Frassoni F, Ball L, et al. Mesenchymal stem cells for treatment of steroid-resistant, severe, acute graft-versus-host disease: a phase II study. Lancet. 2008; 371:1579–1586. [PubMed: 18468541]
12. Horwitz EM, Maziarz RT, Kebriaei P. MSCs in hematopoietic cell transplantation. Biol Blood Marrow Transplant. 2011; 17:S21–29. [PubMed: 21195306]
13. Auletta JJ, Cooke KR, Solchaga LA, et al. Regenerative stromal cell therapy in allogeneic hematopoietic stem cell transplantation: current impact and future directions. Biol Blood Marrow Transplant. 2010; 16:891–906. [PubMed: 20018250]
14. Galipeau J. The mesenchymal stromal cells dilemma--does a negative phase III trial of random donor mesenchymal stromal cells in steroid-resistant graft-versus-host disease represent a death knell or a bump in the road? Cytotherapy. 2013; 15:2–8. [PubMed: 23260081]

15. Schroeder MA, Dipersio JF. Mouse models of graft-versus-host disease: advances and limitations. Dis Model Mech. 2011; 4:318–333. [PubMed: 21558065]
16. Le Blanc K, Ringden O. Immunobiology of human mesenchymal stem cells and future use in hematopoietic stem cell transplantation. Biol Blood Marrow Transplant. 2005; 11:321–334. [PubMed: 15846285]
17. Le Blanc K, Ringden O. Immunomodulation by mesenchymal stem cells and clinical experience. J Intern Med. 2007; 262:509–525. [PubMed: 17949362]
18. Romieu-Mourez R, Coutu DL, Galipeau J. The immune plasticity of mesenchymal stromal cells from mice and men: concordances and discrepancies. Front Biosci (Elite Ed). 2012; 4:824–837. [PubMed: 22201917]
19. Krampera M, Glennie S, Dyson J, et al. Bone marrow mesenchymal stem cells inhibit the response of naive and memory antigen-specific T cells to their cognate peptide. Blood. 2003; 101:3722–3729. [PubMed: 12506037]
20. Di Nicola M, Carlo-Stella C, Magni M, et al. Human bone marrow stromal cells suppress T-lymphocyte proliferation induced by cellular or nonspecific mitogenic stimuli. Blood. 2002; 99:3838–3843. [PubMed: 11986244]
21. Glennie S, Soeiro I, Dyson PJ, et al. Bone marrow mesenchymal stem cells induce division arrest anergy of activated T cells. Blood. 2005; 105:2821–2827. [PubMed: 15591115]
22. Klyushnenkova E, Mosca JD, Zernetkina V, et al. T cell responses to allogeneic human mesenchymal stem cells: immunogenicity, tolerance, and suppression. J Biomed Sci. 2005; 12:47–57. [PubMed: 15864738]
23. Ren G, Zhang L, Zhao X, et al. Mesenchymal stem cell-mediated immunosuppression occurs via concerted action of chemokines and nitric oxide. Cell Stem Cell. 2008; 2:141–150. [PubMed: 18371435]
24. Meisel R, Zibert A, Laryea M, et al. Human bone marrow stromal cells inhibit allogeneic T-cell responses by indoleamine 2,3-dioxygenase-mediated tryptophan degradation. Blood. 2004; 103:4619–4621. [PubMed: 15001472]
25. Cooke KR, Gerbitz A, Crawford JM, et al. LPS antagonism reduces graft-versus-host disease and preserves graft-versus-leukemia activity after experimental bone marrow transplantation. J Clin Invest. 2001; 107:1581–1589. [PubMed: 11413166]
26. Auletta JJ, Zale EA, Welter JF, et al. Fibroblast Growth Factor-2 Enhances Expansion of Human Bone Marrow-Derived Mesenchymal Stromal Cells without Diminishing Their Immunosuppressive Potential. Stem Cells Int. 2011; 2011:235176. [PubMed: 21437189]
27. Silva IA, Olkiewicz K, Askew D, et al. Secondary lymphoid organs contribute to, but are not required for the induction of graft-versus-host responses following allogeneic bone marrow transplantation: a shifting paradigm for T cell allo-activation. Biol Blood Marrow Transplant. 16:598–611. [PubMed: 20117226]
28. Wang F, Dennis JE, Awadallah A, et al. Transcriptional profiling of human mesenchymal stem cells transduced with reporter genes for imaging. Physiol Genomics. 2009; 37:23–34. [PubMed: 19116247]
29. Ganguly S, Ross DB, Panoskaltsis-Mortari A, et al. Donor CD4+ Foxp3+ regulatory T cells are necessary for post-transplantation cyclophosphamide-mediated protection against GVHD in mice. Blood.
30. Quah BJ, Warren HS, Parish CR. Monitoring lymphocyte proliferation in vitro and in vivo with the intracellular fluorescent dye carboxyfluorescein diacetate succinimidyl ester. Nat Protoc. 2007; 2:2049–2056. [PubMed: 17853860]
31. Klopp AH, Gupta A, Spaeth E, et al. Concise review: Dissecting a discrepancy in the literature: do mesenchymal stem cells support or suppress tumor growth? Stem Cells. 2011; 29:11–19. [PubMed: 21280155]
32. Roy D, Steyer GJ, Gargesha M, et al. 3D cryo-imaging: a very high-resolution view of the whole mouse. Anat Rec (Hoboken). 2009; 292:342–351. [PubMed: 19248166]
33. Steyer GJ, Dong F, Kanodia L, et al. Detection and quantification of fluorescent cell clusters in cryo-imaging. Int J Biomed Imaging. 2012; 2012:698413. [PubMed: 22481905]

34. Lyons AB, Doherty KV. Flow cytometric analysis of cell division by dye dilution. Curr Protoc Cytom. 2004; Chapter 9(Unit 9):11. [PubMed: 18770808]
35. Teshima T, Hill GR, Pan L, et al. IL-11 separates graft-versus-leukemia effects from graft-versus-host disease after bone marrow transplantation. J Clin Invest. 1999; 104:317–325. [PubMed: 10430613]
36. Choi SW, Braun T, Chang L, et al. Vorinostat plus tacrolimus and mycophenolate to prevent graft-versus-host disease after related-donor reduced-intensity conditioning allogeneic haemopoietic stem-cell transplantation: a phase 1/2 trial. Lancet Oncol. 2014; 15:87–95. [PubMed: 24295572]
37. Reddy P, Maeda Y, Hotary K, et al. Histone deacetylase inhibitor suberoylanilide hydroxamic acid reduces acute graft-versus-host disease and preserves graft-versus-leukemia effect. Proc Natl Acad Sci U S A. 2004; 101:3921–3926. [PubMed: 15001702]
38. Krijanovski OI, Hill GR, Cooke KR, et al. Keratinocyte growth factor separates graft-versus-leukemia effects from graft-versus-host disease. Blood. 1999; 94:825–831. [PubMed: 10397751]
39. Hill GR, Teshima T, Gerbitz A, et al. Differential roles of IL-1 and TNF-alpha on graft-versus-host disease and graft versus leukemia. J Clin Invest. 1999; 104:459–467. [PubMed: 10449438]
40. Hill GR, Cooke KR, Teshima T, et al. Interleukin-11 promotes T cell polarization and prevents acute graft-versus-host disease after allogeneic bone marrow transplantation. J Clin Invest. 1998; 102:115–123. [PubMed: 9649564]
41. Beilhack A, Schulz S, Baker J, et al. In vivo analyses of early events in acute graft-versus-host disease reveal sequential infiltration of T-cell subsets. Blood. 2005; 106:1113–1122. [PubMed: 15855275]
42. Panoskaltsis-Mortari A, Price A, Hermanson JR, et al. In vivo imaging of graft-versus-host-disease in mice. Blood. 2004; 103:3590–3598. [PubMed: 14715632]
43. Groh ME, Maitra B, Szekely E, et al. Human mesenchymal stem cells require monocyte-mediated activation to suppress alloreactive T cells. Exp Hematol. 2005; 33:928–934. [PubMed: 16038786]
44. Kalinski P. Regulation of immune responses by prostaglandin E2. J Immunol. 2012; 188:21–28. [PubMed: 22187483]
45. Bianco P, Cao X, Frenette PS, et al. The meaning, the sense and the significance: translating the science of mesenchymal stem cells into medicine. Nat Med. 2013; 19:35–42. [PubMed: 23296015]
46. Peister A, Mellad JA, Larson BL, et al. Adult stem cells from bone marrow (MSCs) isolated from different strains of inbred mice vary in surface epitopes, rates of proliferation, and differentiation potential. Blood. 2004; 103:1662–1668. [PubMed: 14592819]
47. Sung JH, Yang HM, Park JB, et al. Isolation and characterization of mouse mesenchymal stem cells. Transplant Proc. 2008; 40:2649–2654. [PubMed: 18929828]
48. Krampera M, Galipeau J, Shi Y, et al. Immunological characterization of multipotent mesenchymal stromal cells-The International Society for Cellular Therapy (ISCT) working proposal. Cytotherapy. 2013
49. Legrand N, Weijer K, Spits H. Experimental models to study development and function of the human immune system in vivo. J Immunol. 2006; 176:2053–2058. [PubMed: 16455958]
50. Yanez R, Lamana ML, Garcia-Castro J, et al. Adipose tissue-derived mesenchymal stem cells have in vivo immunosuppressive properties applicable for the control of the graft-versus-host disease. Stem Cells. 2006; 24:2582–2591. [PubMed: 16873762]
51. Tisato V, Naresh K, Girdlestone J, et al. Mesenchymal stem cells of cord blood origin are effective at preventing but not treating graft-versus-host disease. Leukemia. 2007; 21:1992–1999. [PubMed: 17625609]
52. Tobin LM, Healy ME, English K, et al. Human mesenchymal stem cells suppress donor CD4(+) T cell proliferation and reduce pathology in a humanized mouse model of acute graft-versus-host disease. Clin Exp Immunol. 2013; 172:333–348. [PubMed: 23574329]
53. Chan JL, Tang KC, Patel AP, et al. Antigen-presenting property of mesenchymal stem cells occurs during a narrow window at low levels of interferon-gamma. Blood. 2006; 107:4817–4824. [PubMed: 16493000]
54. Polchert D, Sobinsky J, Douglas G, et al. IFN-gamma activation of mesenchymal stem cells for treatment and prevention of graft versus host disease. Eur J Immunol. 2008; 38:1745–1755. [PubMed: 18493986]

55. Hemmi S, Merlin G, Aguet M. Functional characterization of a hybrid human-mouse interferon gamma receptor: evidence for species-specific interaction of the extracellular receptor domain with a putative signal transducer. Proc Natl Acad Sci U S A. 1992; 89:2737–2741. [PubMed: 1532657]
56. Krampera M. Mesenchymal stromal cell 'licensing': a multistep process. Leukemia. 2011
57. Fuchs EJ. Transplantation tolerance: from theory to clinic. Immunol Rev. 2014; 258:64–79. [PubMed: 24517426]
58. Loewendorf A, Csete M. Concise review: immunologic lessons from solid organ transplantation for stem cell-based therapies. Stem Cells Transl Med. 2013; 2:136–142. [PubMed: 23349327]
59. Szabolcs P, Burlingham WJ, Thomson AW. Tolerance after solid organ and hematopoietic cell transplantation. Biol Blood Marrow Transplant. 2012; 18:S193–200. [PubMed: 22226107]
60. Scandling JD, Busque S, Dejbakhsh-Jones S, et al. Tolerance and withdrawal of immunosuppressive drugs in patients given kidney and hematopoietic cell transplants. Am J Transplant. 2012; 12:1133–1145. [PubMed: 22405058]
61. Leventhal J, Abecassis M, Miller J, et al. Chimerism and tolerance without GVHD or engraftment syndrome in HLA-mismatched combined kidney and hematopoietic stem cell transplantation. Sci Transl Med. 2012; 4:124ra128.
62. Roemeling-van Rhijn M, Khairoun M, Korevaar SS, et al. Human Bone Marrow- and Adipose Tissue-derived Mesenchymal Stromal Cells are Immunosuppressive and in a Humanized Allograft Rejection Model. J Stem Cell Res Ther. 2013; (Suppl 6):20780. [PubMed: 24672744]
63. Vanikar AV, Trivedi HL, Feroze A, et al. Effect of co-transplantation of mesenchymal stem cells and hematopoietic stem cells as compared to hematopoietic stem cell transplantation alone in renal transplantation to achieve donor hypo-responsiveness. Int Urol Nephrol. 2011; 43:225–232. [PubMed: 20084457]
64. Reinders ME, Rabelink TJ, de Fijter JW. The role of mesenchymal stromal cells in chronic transplant rejection after solid organ transplantation. Curr Opin Organ Transplant. 2013; 18:44–50. [PubMed: 23254697]
65. Yanez R, Oviedo A, Aldea M, et al. Prostaglandin E2 plays a key role in the immunosuppressive properties of adipose and bone marrow tissue-derived mesenchymal stromal cells. Exp Cell Res. 2010; 316:3109–3123. [PubMed: 20804749]
66. Chen K, Wang D, Du WT, et al. Human umbilical cord mesenchymal stem cells hUC-MSCs exert immunosuppressive activities through a PGE2-dependent mechanism. Clin Immunol. 2010; 135:448–458. [PubMed: 20207200]
67. Kuci Z, Seiberth J, Latifi-Pupovci H, et al. Clonal analysis of multipotent stromal cells derived from CD271+ bone marrow mononuclear cells: functional heterogeneity and different mechanisms of allosuppression. Haematologica. 2013; 98:1609–1616. [PubMed: 23975178]
68. Rasmusson I, Ringden O, Sundberg B, et al. Mesenchymal stem cells inhibit lymphocyte proliferation by mitogens and alloantigens by different mechanisms. Exp Cell Res. 2005; 305:33–41. [PubMed: 15777785]
69. Solchaga LA, Zale EA. Prostaglandin E2: a putative potency indicator of the immunosuppressive activity of human mesenchymal stem cells. Am J Stem Cells. 2012; 1:138–145. [PubMed: 23087846]
70. Baratelli F, Lin Y, Zhu L, et al. Prostaglandin E2 induces FOXP3 gene expression and T regulatory cell function in human CD4+ T cells. J Immunol. 2005; 175:1483–1490. [PubMed: 16034085]
71. Spaggiari GM, Abdelrazik H, Becchetti F, et al. MSCs inhibit monocyte-derived DC maturation and function by selectively interfering with the generation of immature DCs: central role of MSC-derived prostaglandin E2. Blood. 2009; 113:6576–6583. [PubMed: 19398717]
72. Yamagiwa S, Gray JD, Hashimoto S, et al. A role for TGF-beta in the generation and expansion of CD4+CD25+ regulatory T cells from human peripheral blood. J Immunol. 2001; 166:7282–7289. [PubMed: 11390478]
73. English K, Ryan JM, Tobin L, et al. Cell contact, prostaglandin E(2) and transforming growth factor beta 1 play non-redundant roles in human mesenchymal stem cell induction of CD4+CD25(High) forkhead box P3+ regulatory T cells. Clin Exp Immunol. 2009; 156:149–160. [PubMed: 19210524]

74. Juan G, Jie Y, Guofan C, et al. Xenogeneic Immunosuppression of Human Umbilical Cord Mesenchymal Stem Cells in a Major Histocompatibility Complex (MHC)-mismatched allogeneic acute graft-versus-host disease murine model. Eur J Haematol. 2011

75. Meyerrose TE, De Ugarte DA, Hofling AA, et al. In vivo distribution of human adipose-derived mesenchymal stem cells in novel xenotransplantation models. Stem Cells. 2007; 25:220–227. [PubMed: 16960135]

76. Lee RH, Pulin AA, Seo MJ, et al. Intravenous hMSCs improve myocardial infarction in mice because cells embolized in lung are activated to secrete the anti-inflammatory protein TSG-6. Cell Stem Cell. 2009; 5:54–63. [PubMed: 19570514]

77. Ruster B, Gottig S, Ludwig RJ, et al. Mesenchymal stem cells display coordinated rolling and adhesion behavior on endothelial cells. Blood. 2006; 108:3938–3944. [PubMed: 16896152]

78. Li H, Jiang Y, Jiang X, et al. CCR7 guides migration of mesenchymal stem cell to secondary lymphoid organs: a novel approach to separate GvHD from GvL effect. Stem Cells. 32:1890–1903. [PubMed: 24496849]

79. Dander E, Lucchini G, Vinci P, et al. Mesenchymal stromal cells for the treatment of graft-versus-host disease: understanding the in vivo biological effect through patient immune monitoring. Leukemia. 2012; 26:1681–1684. [PubMed: 22289986]

80. Ball L, Bredius R, Lankester A, et al. Third party mesenchymal stromal cell infusions fail to induce tissue repair despite successful control of severe grade IV acute graft-versus-host disease in a child with juvenile myelo-monocytic leukemia. Leukemia. 2008; 22:1256–1257. [PubMed: 17972946]

81. Prockop DJ. Repair of tissues by adult stem/progenitor cells (MSCs): controversies, myths, and changing paradigms. Mol Ther. 2009; 17:939–946. [PubMed: 19337235]

82. Djouad F, Plence P, Bony C, et al. Immunosuppressive effect of mesenchymal stem cells favors tumor growth in allogeneic animals. Blood. 2003; 102:3837–3844. [PubMed: 12881305]

83. Ljujic B, Milovanovic M, Volarevic V, et al. Human mesenchymal stem cells creating an immunosuppressive environment and promote breast cancer in mice. Sci Rep. 2013; 3:2298. [PubMed: 23892388]

84. Ning H, Yang F, Jiang M, et al. The correlation between cotransplantation of mesenchymal stem cells and higher recurrence rate in hematologic malignancy patients: outcome of a pilot clinical study. Leukemia. 2008; 22:593–599. [PubMed: 18185520]

85. Oviedo A, Yanez R, Colmenero I, et al. Reduced efficacy of mesenchymal stromal cells in preventing graft-versus-host disease in an in vivo model of haploidentical bone marrow transplant with leukemia. Cell Transplant. 2013; 22:1381–1394. [PubMed: 23044223]

86. Sundin M, Barrett AJ, Ringden O, et al. HSCT recipients have specific tolerance to MSC but not to the MSC donor. J Immunother. 2009; 32:755–764. [PubMed: 19561533]

87. Liu K, Chen Y, Zeng Y, et al. Coinfusion of Mesenchymal Stromal Cells Facilitates Platelet Recovery Without Increasing Leukemia Recurrence in Haploidentical Hematopoietic Stem Cell Transplantation: A Randomized, Controlled Clinical Study. Stem Cells Dev. 2011

88. Baron F, Lechanteur C, Willems E, et al. Cotransplantation of mesenchymal stem cells might prevent death from graft-versus-host disease (GVHD) without abrogating graft-versus-tumor effects after HLA-mismatched allogeneic transplantation following nonmyeloablative conditioning. Biol Blood Marrow Transplant. 2010; 16:838–847. [PubMed: 20109568]

89. Bernardo ME, Fibbe WE. Mesenchymal stromal cells: sensors and switchers of inflammation. Cell Stem Cell. 2013; 13:392–402. [PubMed: 24094322]

90. Prockop DJ, Oh JY. Mesenchymal stem/stromal cells (MSCs): role as guardians of inflammation. Mol Ther. 2012; 20:14–20. [PubMed: 22008910]

91. Chinnadurai R, Copland IB, Patel SR, et al. IDO-independent suppression of T cell effector function by IFN-gamma-licensed human mesenchymal stromal cells. J Immunol. 192:1491–1501. [PubMed: 24403533]

92. Mellor AL, Munn DH. IDO expression by dendritic cells: tolerance and tryptophan catabolism. Nat Rev Immunol. 2004; 4:762–774. [PubMed: 15459668]

93. Kang KN, Kim da Y, Yoon SM, et al. Tissue engineered regeneration of completely transected spinal cord using human mesenchymal stem cells. Biomaterials. 2012; 33:4828–4835. [PubMed: 22498301]

94. Li Y, Lin F. Mesenchymal stem cells are injured by complement after their contact with serum. Blood. 2012; 120:3436–3443. [PubMed: 22966167]

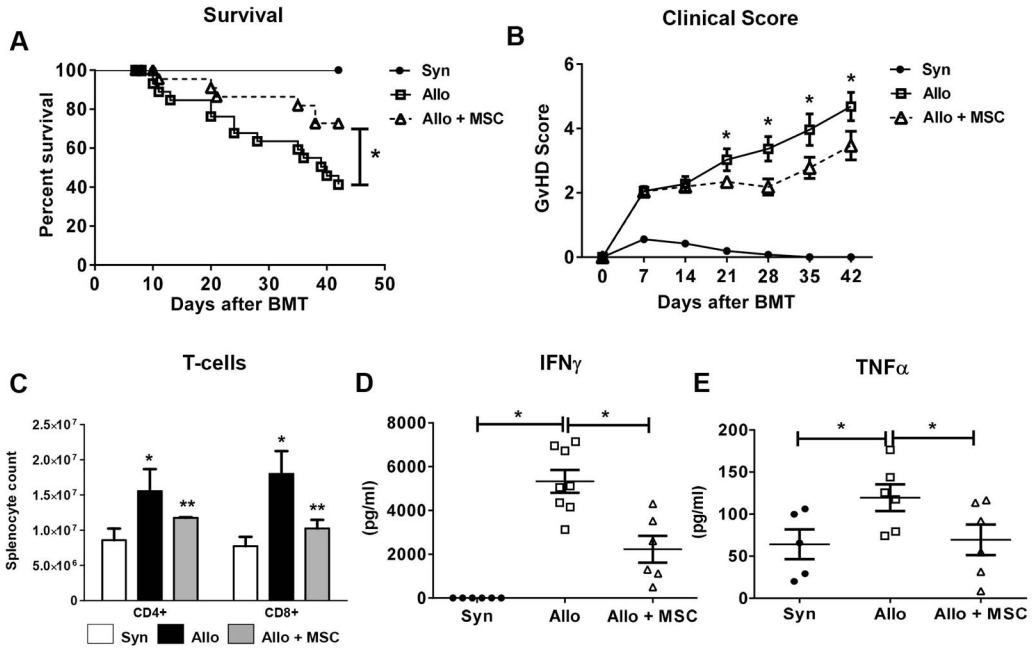

Figure 1. Human MSC infusions (hMSCs) regulate *in vivo* T-cell expansion, pro-inflammatory cytokine secretion and systemic GvHD following alloBMT

(A) hMSC infusions reduce systemic GvHD following alloBMT as measured by survival. Data are expressed as mean ± SEM and represent three combined transplant experiments [(n= 15 to 30 mice per experimental group; * $p < 0.05$ allo control vs. allo + MSC by Mantel-Cox log-rank test (survival) and unpaired t-test (clinical score)]. **(B)** hMSC infusions improve clinical GvHD scores in alloBMT mice. Combined clinical scores (mean ± SEM) from three separate transplant experiments are depicted. Asterisks (*) indicate significant differences in mean clinical GvHD scores between indicted alloBMT groups at listed post-transplant times ($p<0.05$, unpaired t-test). **(C)** hMSC infusions result in decreased donor T-cell expansion at D10. Data are expressed as mean ± SEM and are from one of three representative independent experiments (n=3 to 6 mice per group; * $p < 0.05$ syn vs. allo control; ** $p < 0.05$ allo control vs. allo + MSC by Mann-Whitney test). **(D, E)** AlloBMT mice receiving MSC infusions have decreased levels of circulating IFNγ (D) and TNFα (E). Whole blood was collected, serum separated and ELISA used to measure cytokine levels from individualized mice at D7 (IFNγ) and D10 (TNFα). Data are expressed as mean ± SEM and are from one of three independent experiments (n=5 to 6 mice per experimental group; * $p < 0.05$ for indicated comparisons by Mann-Whitney test).

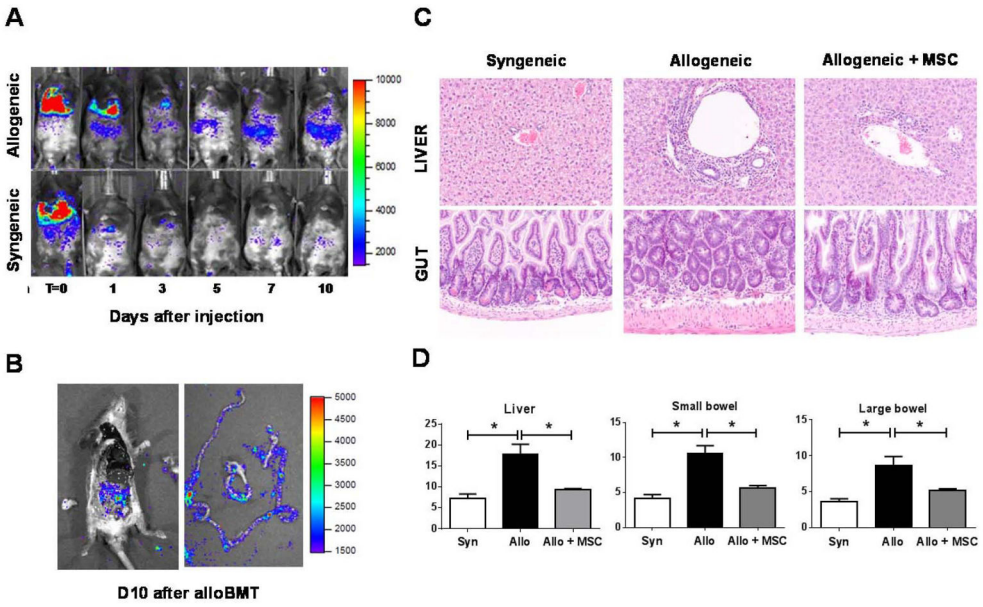

Figure 2. hMSCs migrate to abdominal organs and attenuate target-tissue GvHD cytotoxicity

(A) Serial bioluminescence imaging (BLI) demonstrates that hMSCs home to the gastrointestinal tract in alloBMT mice. Data from one of three similar independent experiments is shown. (**B**) Post-mortem examination of intestines dissected from alloBMT mice that received hMSC infusions on D1 and D4. The mouse was euthanized and abdominal tissues dissected on D10. BLI was performed on dissected intestines. **(C, D)** Early reduction in proinflammatory T-cell expansion and cytokine induction as shown in Figure 1 associates with decreases in GvHD-associated histopathology in liver and bowel (C) and reduced GvHD organ histology scores (D). Organs harvested from five individual mice per transplant group were analyzed for GvHD severity at D10. Data are expressed as mean ± SEM and represent one of two similar experiments (n=5 mice per experimental group; * $p < 0.01$ and ** $p < 0.05$ for indicated comparisons by Mann-Whitney test).

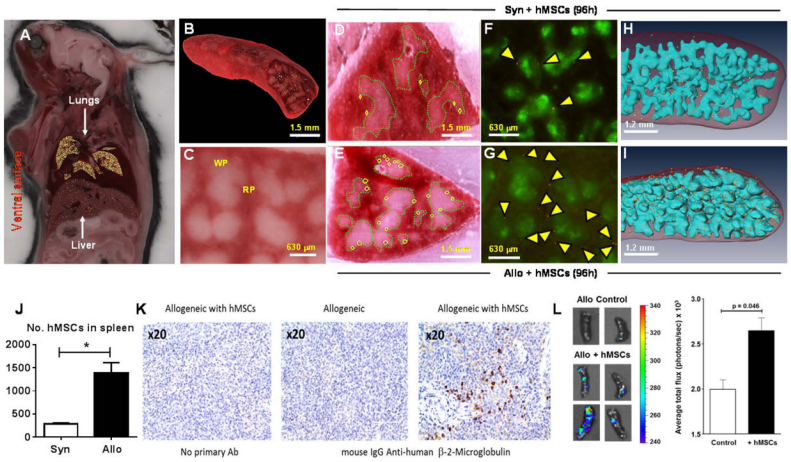

Figure 3. Bio-distribution of hMSCs and murine T-cells (mTCs) within allogeneic and syngeneic transplant-recipient spleens

(A, B) Using cryo-imaging red Qdot-labeled hMSCs (rendered in gold) appear initially in the lung (A) and liver 6 h after tail-vein injection on D1 after BMT and then migrate to spleen in both syngeneic (not shown) and allogeneic (shown) BMT recipient mice by 24 h post-injection (D2 after BMT, cells are visible in the cut-away when zoomed) (B). **(C)** Bright field imaging shows splenic white ("WP") and red ("RP") pulp architecture. **(D, E)** Marginal zones in syngeneic (D) and allogeneic (E) animals are outlined as dotted green lines 96 h post hMSC (yellow shapes) infusion. **(F, G)** Fluorescent imaging at 96 h shows green CFSE-labeled mTCs in white pulp regions and red hMSCs within the marginal zones in both syngeneic (F) and allogeneic (G) transplant mice. **(H, I)** Three-dimensional (3D) rendering of WP shows that less hMSCs (gold beads) localize to the marginal zone following syngeneic (H) than after allogeneic (I) BMT. **(J)** Numbers of hMSCs homing to the spleen in allogeneic and syngeneic transplant mice were quantified after 96 h post-MSC infusion. Data are presented as mean ± SEM and represent one of two independent and similar experiments (n=3 mice per experimental group, per time point; * $p < 0.05$ for indicated comparisons by Mann-Whitney test). (**K, L**) The presence of hMSCs in the spleen was confirmed by IHC using a monoclonal anti-human antibody to β-2-microglobulin (K) and semi-quantitative BLI (L). Representative photomicrographs are shown from one of three IHC slides per experimental group. BLI data are representative of 4 mice per experimental group, * $p = 0.05$, for indicated comparisons by Mann-Whitney test).

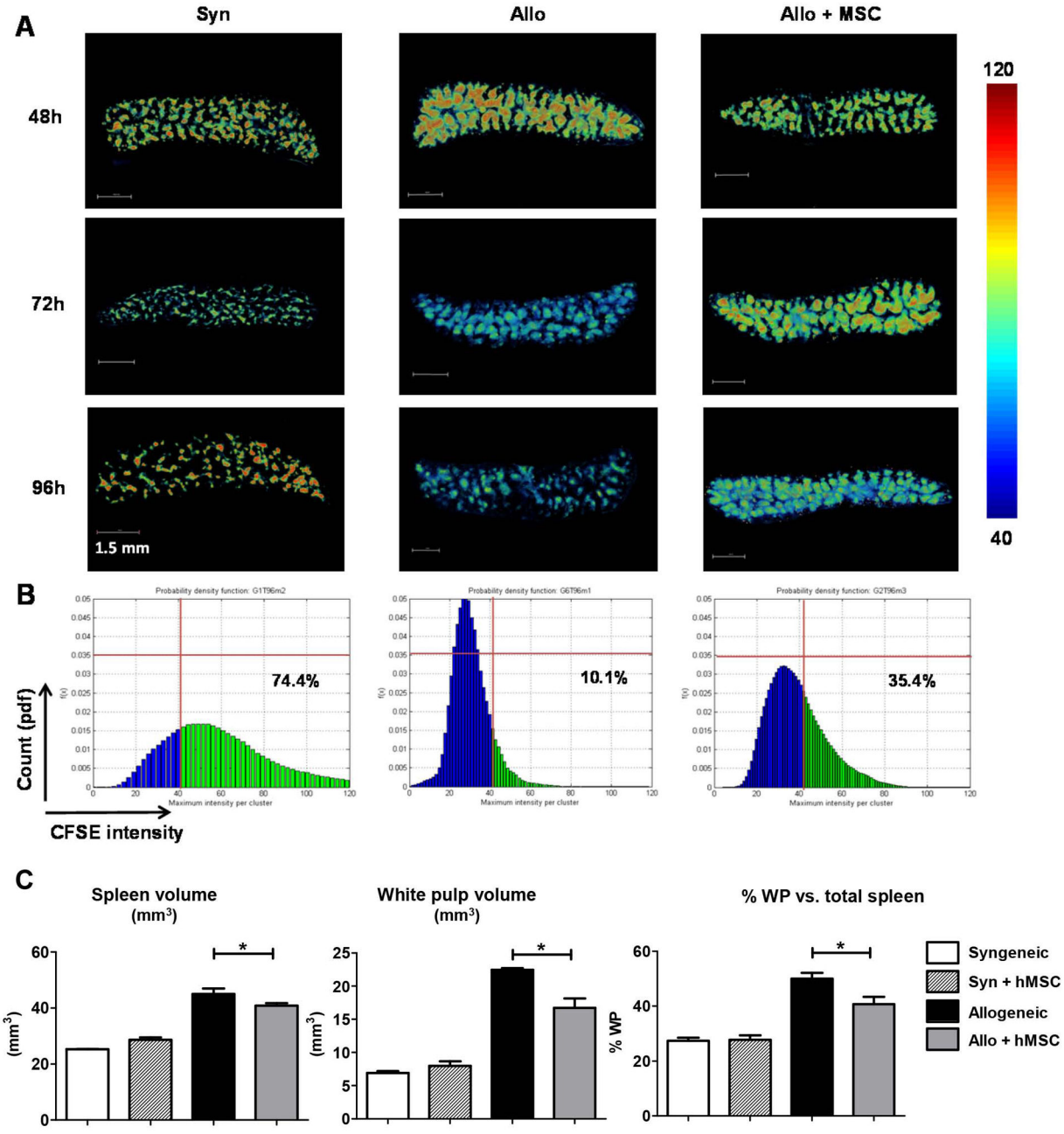

Figure 4. Labeled mTCs in alloreactive mice retain CFSE intensity in alloBMT mice receiving hMSCs

(A) Volume rendering of CFSE fluorescence shows WP distribution of mTCs in syngeneic ("syn"), allogeneic ("allo"), and hMSC-infused allogeneic spleens ("allo + MSC") at indicated time points post-transplant. **(B)** Probability density function (PDF) of CFSE fluorescence intensity per cell was used to estimate the fraction of bright mTCs over all detected mTCs. Green-shaded areas in histograms represent the percentages of mTC that retain high CFSE intensity (low mTC proliferation), while blue-shaded areas represent percentages of mTCs with low CFSE intensity (high mTC proliferation). Each

representative histogram is from an individual mouse within the indicated experimental group (n=3 mice per experimental group). Data from one of two independent experiments is shown. **(C)** Quantitative analyses of spleen and white pulp volumes (in mm^3) and the fraction of WP to total splenic volume (in %) are shown (n=3 mice per experimental group per time point; * $p = 0.05$, for indicated comparisons by Mann-Whitney test).

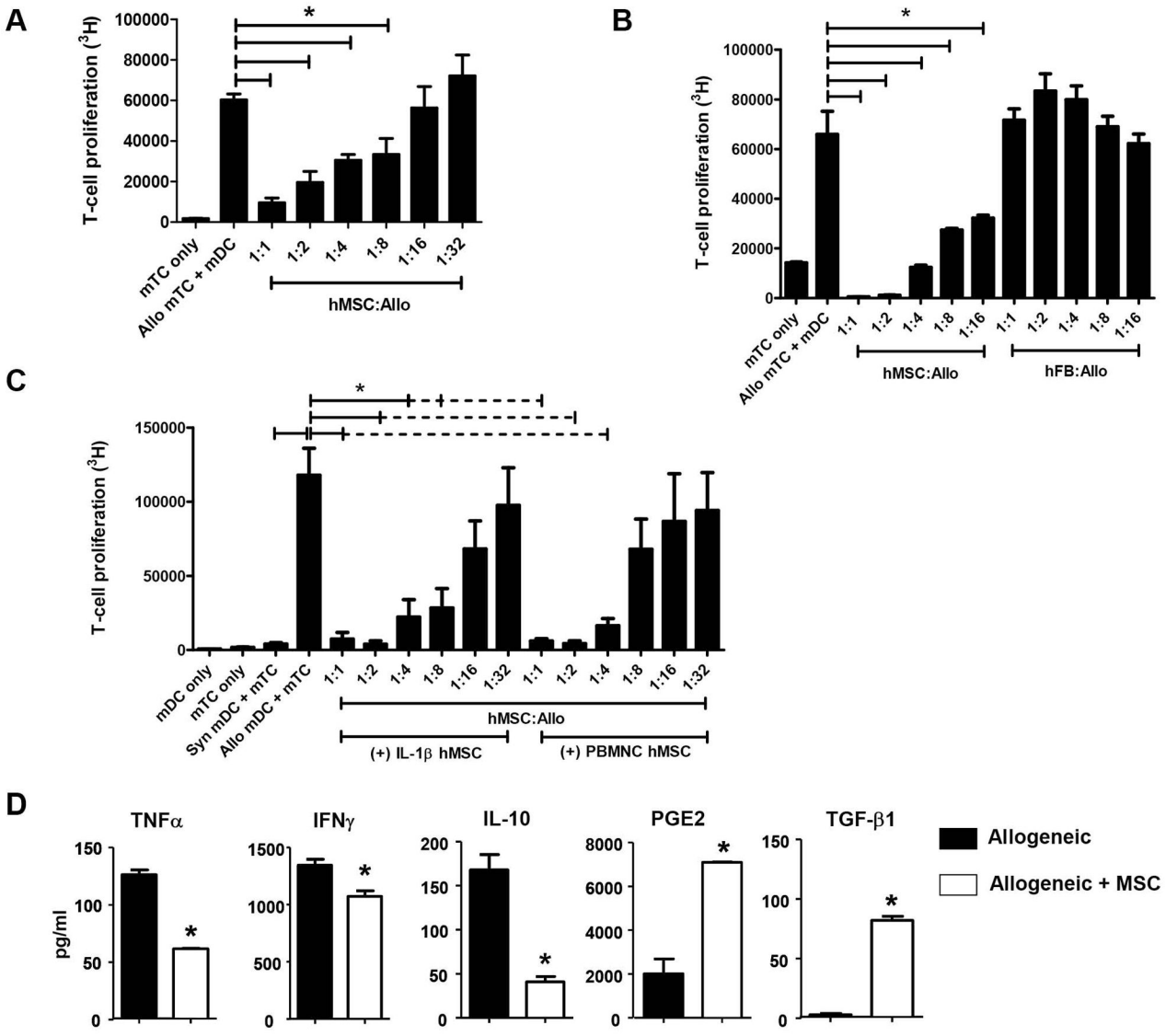

Figure 5. Human MSCs modulate *in vitro* mTC alloreactivity *in vitro*

(A) hMSCs inhibit murine T-cell alloreactivity in a dose-dependent fashion. **(B)** MSCs are unique stromal cells that mediate inhibition of murine T-cell alloreactivity. Mixed leukocyte cultures (MLCs) were prepared as described above using human fibroblasts (hFB) in indicated hFB-to-mTC ratios. **(C)** MSCs stimulated with either human IL-β (10 pg/ml) or 20,000 human PBMCs inhibit *in vitro* T-cell alloreactivity. **(D)** MSC-mediated suppression of *in vitro* mTC proliferation correlates with changes in T-cell cytokine production. mTC proliferation **(A, B, C)**, cytokine production and surface T-cell activation expression (D) were measured in triplicate from one of three to four independent experiments using hMSCs from different donors. Data are expressed as means ± SEM (* $p < 0.05$ and ** $p < 0.001$ for indicated comparisons by Mann-Whitney test).

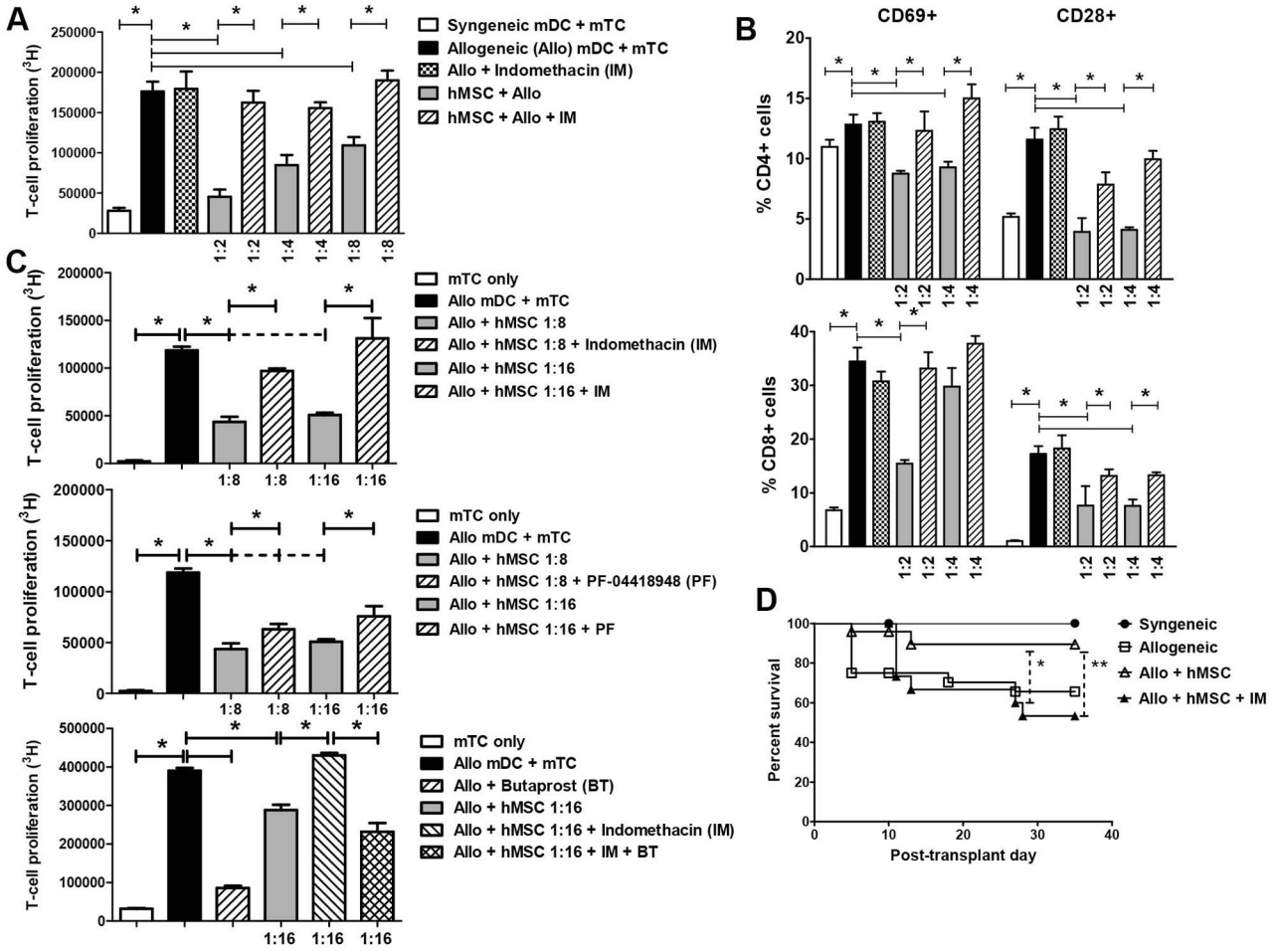

Figure 6. PGE_2 mediates the immunomodulatory effects of hMSCs on T-cell alloreactivity

(A, B) Indomethacin reverses MSC-mediated inhibition of mTC proliferation (A) and surface activation markers (B). B6 splenic mTCs were co-cultured with syngeneic (B6) and allogeneic (B6D2F1) splenic-derived DCs in the presence or absence of hMSCs at indicated hMSC-to-mTC ratios. Indomethacin (IM, 1 μg/ml) or diluents was added to some co-culture wells. Mouse $CD4^+$ and $CD8^+$ T-cells were collected after 72h, stained with fluorescently-labeled conjugate antibodies and analyzed by flow cytometry for cell surface expression of CD28 and CD69. Data are expressed as mean ± SEM from one of at least two independent experiments (* $p < 0.05$ for indicated comparisons by Mann-Whitney test). **(C)** Effects of hMSC-mediated on TC alloreactivity are both COX- and EP2-dependent, suggesting that PGE_2 is necessary and sufficient in mediating hMSC TC immunomodulation. EP2 antagonism reverses hMSC-mediated TC attenuation albeit not to the same degree as COX inhibition. The EP2 antagonist, PF-04418948 (PF, 2 μg/ml), IM (1 μg/ml) and the EP2 agonist, butaprost (BT, 2 μg/ml), were added to defined hMSCs-to-TC ratios and subsequent TC proliferation at 72 h was measured. Each indicated condition was measured in triplicate, and results shown are from one of two independent experiments (* $p < 0.05$ for indicated comparisons by Mann-Whitney test). **(D)** In addition to 1M hMSCs via tail-injection on D1 and D4, allogeneic transplant recipient mice also received 20 μg indomethacin (IM) via

intraperitoneal injection on Days 1–7 post-BMT. Data shown are combined results from two separate independent transplant experiments. (n = 8 to 12 mice per group, * $p < 0.05$ and ** $p < 0.05$ by Mann-Whitney test for indicated percent survival comparisons between “Allo + hMSC” and “Allo + hMSC + IM” at D28 and D35, respectively).

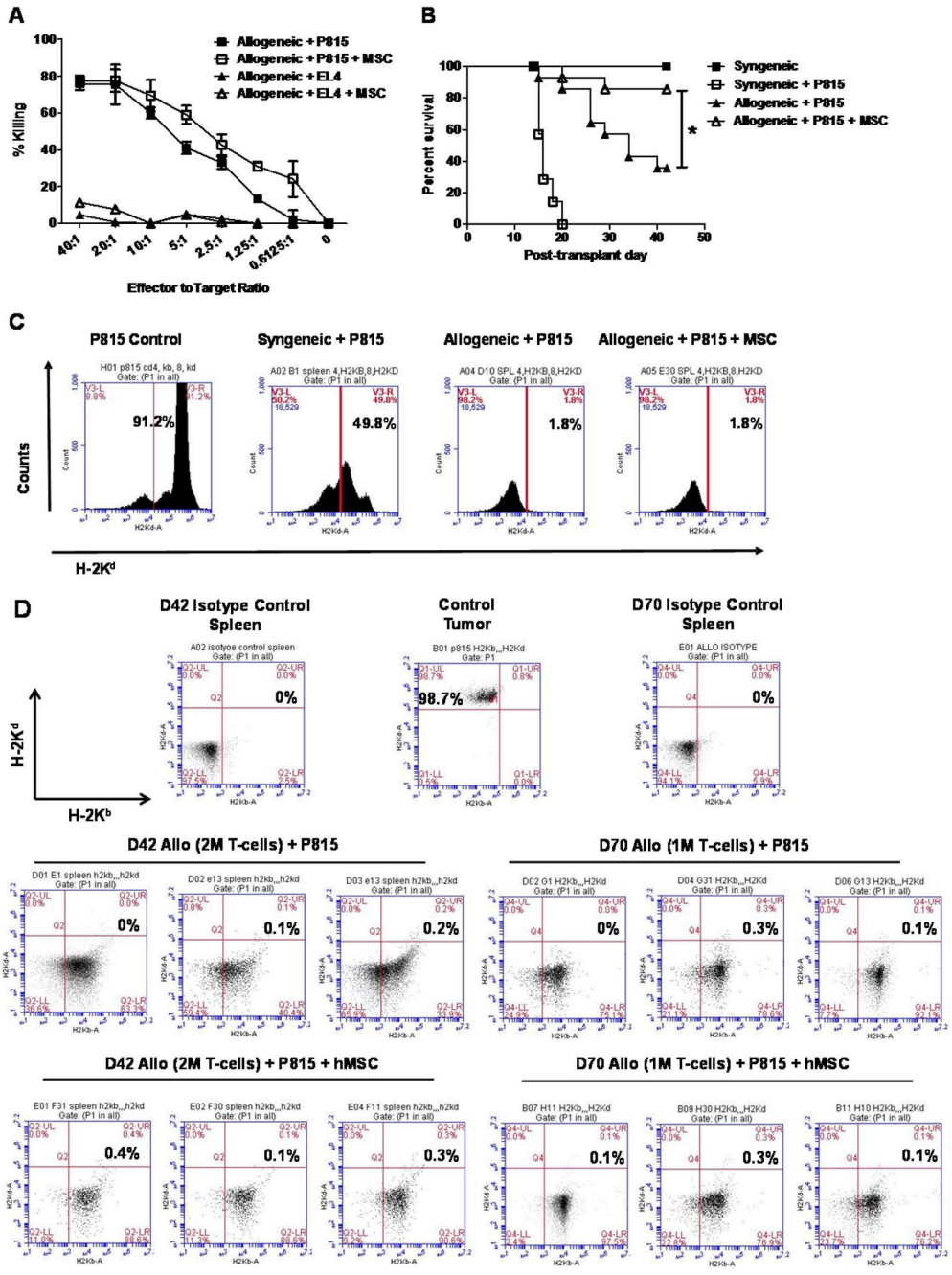

Figure 7. MSCs infusions preserve *in vitro* cytotoxic T-lymphocyte (CTL) activity and prolong survival in alloBMT following *in vivo* leukemic challenge

(A) MSCs do not interfere with *ex vivo* CTL-directed against P815 tumor cells. Allogeneic B6 T cells were stimulated in bulk by splenic-derived B6D2F1 DCs with or without hMSCs at a MSC-to-mTC ratio of 1:4. CTLs were subsequently isolated using Ficoll gradient and co-cultured with either P815 (H-2K^d) or EL4 (H-2K^b) tumor cell lines and cytolytic activity. Data are expressed as mean ± SEM and represent one of two similar, independent experiments. **(B, C)** MSC infusions preserve alloreactive graft-versus-leukemia (GvL) activity in alloBMT mice following P815 challenge as measured by survival (B) and

minimal residual disease (MRD) using flow cytometry (C). Data from one of two independent experiments is shown. (n=8 to 16 mice per group; $*p < 0.05$ allo controls + P815 vs. allo + P815 + MSC by Mantel-Cox log-rank test). **(D)** GvL activity is preserved late post-transplant (D42) following hMSC infusions in allogeneic transplant mice challenged with P815 at lower T-cell doses (D70). AlloBMT mice received either one (1M) or two (2M) million B6 TCs on D0 and then 1M hMSCs or diluent only via tail-vein injection on D1 and D4. Representative FACS dot plots of H-2K^d-stained splenocytes from individual mice from two independent experiments are shown. Data for syngeneic mice were obtained at D14 given that syngeneic mice challenged with P815 uniformly die from tumor by D21.